Decontamination

Deutsche Ausgabe: DOI: 10.1002/ange.201601620
Internationale Ausgabe: DOI: 10.1002/anie.201601620

Broad-Spectrum Liquid- and Gas-Phase Decontamination of Chemical Warfare Agents by One-Dimensional Heteropolyniobates

*Weiwei Guo, Hongjin Lv, Kevin P. Sullivan, Wesley O. Gordon, Alex Balboa, George W. Wagner, Djamaladdin G. Musaev, John Bacsa, and Craig L. Hill**

Abstract: *A wide range of chemical warfare agents and their simulants are catalytically decontaminated by a new one-dimensional polymeric polyniobate (P-PONb), $K_{12}[Ti_2O_2][GeNb_{12}O_{40}]\cdot 19H_2O$ (**KGeNb**) under mild conditions and in the dark. Uniquely, **KGeNb** facilitates hydrolysis of nerve agents Sarin (GB) and Soman (GD) (and their less reactive simulants, dimethyl methylphosphonate (DMMP)) as well as mustard (HD) in both liquid and gas phases at ambient temperature and in the absence of neutralizing bases or illumination. Three lines of evidence establish that **KGeNb** removes DMMP, and thus likely GB/GD, by general base catalysis: a) the $k(H_2O)/k(D_2O)$ solvent isotope effect is 1.4; b) the rate law (hydrolysis at the same pH depends on the amount of P-PONb present); and c) hydroxide is far less active against the above simulants at the same pH than the P-PONbs themselves, a critical control experiment.*

Chemical warfare agents (CWAs), used in past wars and recent terrorist attacks, represent a significant threat to humankind.[1] Among all of the classes of chemical weapons, vesicants (such as sulfur mustard) and nerve agents are the most common.[2] Sulfur mustard is one of the most effective CWAs used in modern warfare.[3] Nerve agents are organophosphorus compounds containing P–X bonds (X = F, CN, SR etc.),[4] that rapidly inactivate acetylcholinesterase, the enzyme which facilitates hydrolysis of the neurotransmitter acetylcholine in the nervous system, leading to a range of incapacitating states and in higher concentrations, death.[5] There remains a need to develop materials and methods to rapidly, fully and catalytically decontaminate all the main CWAs under mild conditions.

Both organic and inorganic materials have been developed to catalyze hydrolysis of nerve agents and their simulants.[2,6] A series of Zr-based metal-organic frameworks (MOFs, especially UiO-66, NU-1000 and MOF-808) that contain strongly acidic Zr^{IV} sites, have shown significant catalytic activities for hydrolyzing nerve agents and the simulant dimethyl 4-nitrophenyl phosphate (DMNP).[7] However, the catalytic hydrolysis of DMNP by the Zr-based MOFs often requires the addition of *N*-ethylmorpholine as a buffer and a proximal base. These MOFs are of low activity decontaminating the relatively inert nerve agent simulant, DMMP.[8] Recently, a porphyrinic MOF that catalyzes selective photooxidation of a sulfur mustard simulant was also reported.[9]

Polyoxometalates (POMs), one polyoxoniobate (PONb), $[Nb_6O_{19}]^{8-}$ and other Nb-based solid materials have also been investigated for the degradation of CWAs and/or their simulants.[10] POMs are a class of metal oxide clusters with versatile applications in magnetism, medicine, electrochemistry and catalysis.[11] PONbs are a subclass of POMs with high negative charges per polyanion oxygen and commensurately basic surface oxygens.[12] We report here that a heterogeneous one-dimensional polymeric heteropolyniobate: $K_{12}[Ti_2O_2][GeNb_{12}O_{40}]\cdot 19H_2O$ (**KGeNb**) is as effective as any basic heterogeneous CWA hydrolysis catalyst to date and the mechanism is probed by kinetics and other methods.

In 2002, Nyman and co-workers reported the single crystal structure of $K_{12}[Ti_2O_2][SiNb_{12}O_{40}]\cdot 22H_2O$ (**KSiNb**).[13] In 2005, the structures of the sodium salts of $[Ti_2O_2][SiNb_{12}O_{40}]^{12-}$ and $[Ti_2O_2][GeNb_{12}O_{40}]^{12-}$ were inferred from PXRD data.[14] However, given the remarkable basic reactivity of these one-dimensional polyniobates, we sought a high-resolution single-crystal structural determination of these nano-thread-like materials in order to facilitate more detailed experimental and computational study of their surface-related reactions.

Although significant efforts failed to produce single crystals of the sodium salt of the germanium-based heteropolyanion, $[Ti_2O_2][GeNb_{12}O_{40}]^{12-}$, the corresponding potassium salt, **KGeNb**,[15] was readily synthesized under hydrothermal conditions from $Nb_2O_5\cdot xH_2O$, tetraethoxygermane and tetraisopropyltitanium in an aqueous solution of KOH. Not surprisingly considering the similar size and properties of the Ge^{IV} and Si^{IV} heteroatoms, **KGeNb** and **KSiNb** are isostructural. These nano-scale threads are composed of silico/germano-dodecaniobate Keggin ions connected by two edge-sharing TiO_6 octahedra ($[Ti_2O_2]^{4+}$) forming one-dimensional infinite chains (Figure 1 a).[14] The K^+ counter cations are situated between the 1D polyanions, and Figure 1 b shows that two of the K^+ ions reside in pockets defined by adjacent Keggin units in each polyanion polymer. The rate of nerve agent decomposition by $[Nb_6O_{19}]^{8-}$ is affected by counter cations.[10a] Although the specific counter cation effect in **KGeNb** is complicated, the short bond lengths

[*] W. Guo, K. P. Sullivan, Dr. D. G. Musaev, Prof. C. L. Hill
Department of Chemistry, Cherry L. Emerson Center for Scientific Computation, Emory University
1515 Dickey Dr., Atlanta, Georgia 30322 (USA)
E-mail: chill@emory.edu
W. Guo, K. P. Sullivan, Dr. J. Bacsa, Prof. C. L. Hill
X-ray Crystallography Center, Emory University
1515 Dickey Dr., Atlanta, Georgia 30322 (USA)
W. O. Gordon, A. Balboa, G. W. Wagner
U.S. Army Edgewood Chemical Biological Center
APG, MD 21010-5424 (USA)

Supporting information for this article can be found under: http://dx.doi.org/10.1002/anie.201601620.

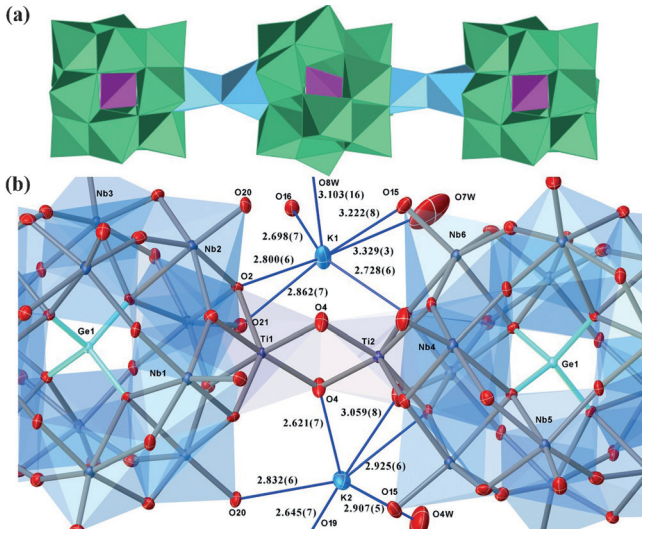

Figure 1. a) Polyhedral representation of the one-dimensional polyanion chain of **KGeNb**. Color code: green: NbO_6; blue: TiO_6; pink: GeO_4. b) Precise structural environments of two potassium counter cations interacting with the polymeric polyanion unit (bond lengths in Å)

(2.621–3.329 Å) including one to the Ti-O-Ti oxygen (O4 from the X-ray structure) implicates a non-innocent role for these counter cations in the organophosphate compound degradation mechanism.

The U.S. Army nominated DMMP as an ideal model chemical for toxicology and carcinogenesis studies.[8] In this study, **KSiNb** and the new more reactive P-PONb, **KGeNb**, hydrolyze DMMP to methyl phosphonic acid (MP) under mild conditions (with only water at room temperature (Figure 2a and 2b). Hydrolysis of the phosphate ester bonds was observed and monitored by ^{31}P NMR spectroscopy (Figure S4 in the Supporting Information (SI)). The extent of conversion was calculated as the ratio of the integrated ^{31}P NMR peak for MP (the only hydrolysis product) to that of DMMP. **KGeNb** converts 54% of this quite inert simulant over the time course of 264 h. The rates of DMMP hydrolysis by **KGeNb** or **KSiNb** slow down after ca. 100 h due to the production of MP which inhibits the reaction (Figure S5).

The higher hydrolytic activity of **KGeNb** relative to **KSiNb** could be explained by a) smaller crystallites of the former than the latter, b) slight dissolution of these P-PONbs to form hydrolytically active soluble monomeric polyniobate species, with **KGeNb** being slightly more soluble than **KSiNb**, or c) an intrinsically more reactive polymeric polyanion for **KGeNb** than for **KSiNb**. Scenario (a) is not likely because examination of **KGeNb** and **KSiNb** by optical microscope shows similar crystallite sizes for both (Figure S6). Furthermore, both of these P-PONbs were ground to make particles that were smaller and quite uniform prior to use in the decontamination reactions. Scenario (b) is very unlikely from five lines of evidence: 1) there is no detectable activity in the supernatant after suspensions of **KGeNb** or **KSiNb** are used for DMMP hydrolysis (the suspensions were filtered and the filtrate assessed for activity after use; Figure S7); 2) elemental analysis of the filtrate indicates negligible amounts of Si, Nb or Ge are present; 3) the weighable amount of **KGeNb** and **KSiNb** is the same before and after reaction; 4) the **KGeNb** collected after reaction, washed extensively with deionized water, dried under vacuum and re-used in successive DMMP hydrolysis runs shows comparable activity to the first run (Figure S8); and 5) the FT-IR of **KGeNb** and **KSiNb** before and after the reaction with DMMP remain identical (Figures S9 and S10). All these argue for the heterogeneous nature of the catalytic hydrolysis. Thus, scenario (c) is possible and might derive from the subtle effects on the negative charge density of the polyanion oxygens by larger size of the central GeO_4 tetrahedron versus the central SiO_4 tetrahedron.

The initial rate for reaction of DMMP with **KGeNb** is approximately first order with respect to DMMP (Figures S11) and the quantity of insoluble **KGeNb** present (at constant pH 10, Figures S12), which is strong evidence for

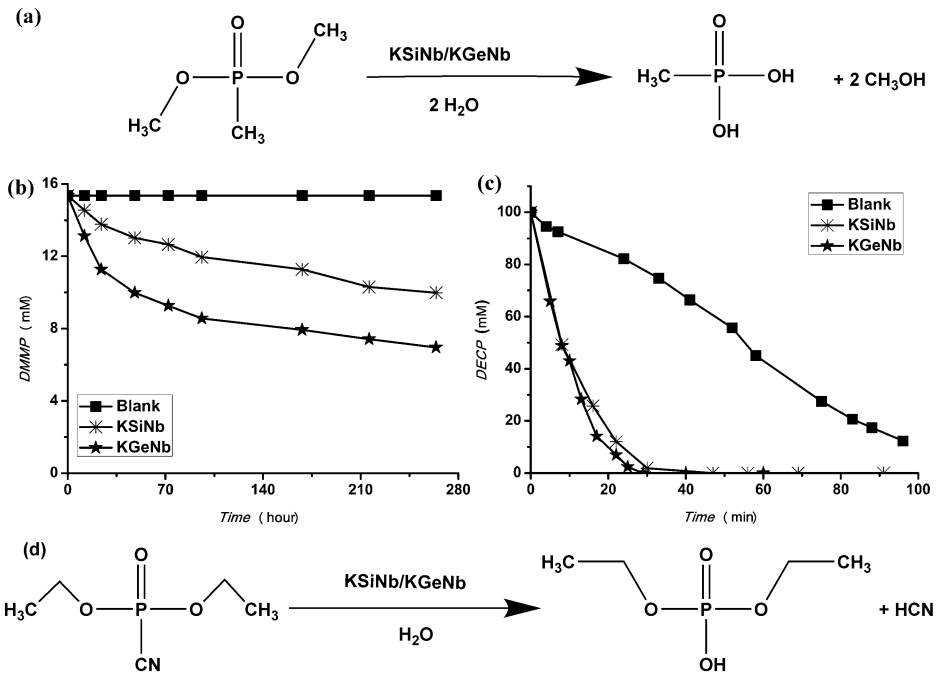

Figure 2. a) Hydrolytic decomposition pathway of DMMP to MP. b) DMMP decomposition using **KGeNb** and **KSiNb**; conditions: [DMMP] = 15.5 mM, 18 μmol **KGeNb** or **KSiNb**, 0.5 mL D_2O and 1.0 mL H_2O at room temperature. c) DECP decomposition using **KGeNb** and **KSiNb**; conditions: [DECP] = 100 mM, 11 μmol **KGeNb** or **KSiNb**, 600 μL of DMF and 50 μL of H_2O at room temperature. d) Hydrolytic decomposition pathway of DECP to DEHP.

a general base-catalyzed mechanism. We note the well-established qualification that getting the order in a heterogeneous catalyst is subject to more error than for homogeneous reactants where the concentration is precisely defined. We also measured the kinetic solvent isotope effect for DMMP hydrolysis.[16] The ratio of reaction rate constants, $k(H_2O)/k(D_2O)$, was determined to be 1.4, which is also consistent with a general base-catalyzed reaction.[17] A third argument for general base catalysis is that the rate of DMMP hydrolysis by hydroxide alone is far lower than by P-PONbs at that same pH (pH 10) (Table 1). The collective data indicate that

Table 1: Comparison of DMMP and DECP decomposition by different materials at room temperature under the same conditions.[a]

Materials	Substrate	Time	Conversion	$t_{1/2}$ [h]
KGeNb	DMMP	24 h	25%	54
UiO-66	DMMP	24 h	<1%	>1343
MOF-808	DMMP	24 h	<1%	>1343
NaOH[b]	DMMP	24 h	4%	336
$K_8Nb_6O_{19}$	DMMP	24 h	5%	269
KGeNb	DECP	30 min	100%	0.1
UiO-66	DECP	30 min	32%	1.3
MOF-808	DECP	30 min	50%	0.4
$K_8Nb_6O_{19}$	DECP	30 min	90%	0.2
MgO	DECP	30 min	90%	0.2
TiO_2	DECP	30 min	87%	0.2
KSiNb	GD	1 h	43%	1.2
$Cs_8Nb_6O_{19}$	GD	1 h	37%	1.4
N/A[c]	GD	1 h	<1%	31

[a] Conditions for DMMP hydrolysis: [DMMP] = 15.5 mM, 50 mg of materials for each entry, 0.5 mL D_2O and 1.0 mL H_2O. Conditions for DECP hydrolysis: [DECP] = 100 mM, 30 mg of material for each entry, 600 μL of DMF and 50 μL of H_2O. [b] NaOH was prepared as a homogeneous phase with a pH of 10. [c] No MOF, POM or other active material added.

generation of hydroxide by reaction of the P-PONb with water in an initial pre-equilibrum (specific base catalysis) does not account for the great majority of the nerve agent simulant hydrolysis by these basic polymeric nano-scale thread-like materials. A general-base hydrolysis mechanism dictates that the slow step of the overall hydrolysis mechanism involves deprotonation of a water molecule by the P-PONb while the incipient forming hydroxide simultaneously attacks its electrophilic partner, the nerve agent simulant phosphorus atom. This is also consistent with the mechanism proposed for the decomposition of diisopropyl fluorophosphates by $[Nb_6O_{19}]^{8-}$.[10a] The subsequent charge neutralization of product species by proton transfer is fast and does not contribute to the observed rate.

Figure 2c and 2d show the time profile and the reaction pathway for the hydrolytic degradation of another CWA simulant, diethyl cyanophosphonate (DECP) to diethyl hydrogen phosphate (DEHP) by **KGeNb** and **KSiNb**. Hydrolysis of the P-CN bond was observed and monitored by ^{31}P NMR spectroscopy. Within 30 min, all DECP is removed. The addition of **KGeNb** or **KSiNb** to the mixture greatly accelerates the reaction. A TON of ca. 6 is achieved in 30 min. Without addition of extra base to remove the acidic and thus self-inhibiting hydrolysis product, nor with strong mixing or other means to increase the TON, this level of reactivity under ambient conditions is of interest for human protection in some real-world environments. Keep in mind that the deployed decontaminating technologies in use by the U.S. Army are essentially stoichiometric. Any catalytic method that could use ambient water (humid air) for hydrolysis or ambient O_2 (air) for oxidative decontamination remains of considerable interest. **KGeNb** and **KSiNb** both contain many water of hydration (hydrogen-bonded to the basic polyniobate oxygens) and thus should be able to catalytically remove many equivalents of nerve agent per repeating unit in their as-synthesized forms.

Table 1 summarizes the activities of **KGeNb**, the reported Zr-based MOFs, the monomeric polyniobate, $[Nb_6O_{19}]^{8-}$, as well as simple hydroxide, against DMMP and DECP under the same mild conditions. The half-life, $t_{1/2}$ (50% conversion) is also listed.[6m] UiO-66 or MOF-808 show no detectable hydrolysis of DMMP under the same conditions, although under other conditions some of these MOFs do hydrolyze DMMP.[7c] Control experiments using Nb_2O_5, NbO_2, TiO_2 or MgO show no degradation of DMMP whatsoever,[2c] and a lower activity towards DECP by MgO or TiO_2 compared with **KGeNb** is observed (Table 1). **KGeNb** is also more active than $[Nb_6O_{19}]^{8-}$ towards DMMP or DECP under the same conditions. Since the P-PONbs under the reaction conditions in this study are effectively insoluble, the local negative changes of the polymeric polyanions consequently appear to be vital for efficient basic nerve agent simulant hydrolysis.

KSiNb was investigated for its activity towards the degradation of live agent, GD (Table 1 and Figure S13). After 1 h, 43% of the GD is consumed with continuous stirring, a point consistent with the oxygens of this polymer being more reactive those those of $[Nb_6O_{19}]^{8-}$. The control reaction (same conditions but no P-PONb added) shows negligible reaction of GD within 1 h. Degradation of GB by **KGeNb** and **KSiNb** was also studied in the gas phase (GB vapor passed over the P-PONb) using diffuse reflectance infrared Fourier transform spectroscopy (DRIFTS). Figures S14 and S15 indicate that GB is partially hydrolyzed on **KGeNb** and **KSiNb** at room temperature (see SI for details and spectral characterization).

KGeNb and **KSiNb** were also investigated for the degradation of HD using DRIFTS (Figure 3 and S16). Difference IR spectra collected in situ of the **KGeNb** during HD exposure did not show peaks associated with intact HD adsorbed to the surface of the material. Instead, perturbation of water molecules and/or hydroxo groups of **KGeNb** and **KSiNb** was noted by a negative feature at 3630 cm^{-1}. A multiplet of peaks was observed from 1230 to 1050 cm^{-1} which likely derives from the formation of the hydrolysis products: half mustard (HM) and thiodiglycol (TDG). Negative peaks in the 930–820 cm^{-1} range are due to depletion of modes of **KGeNb** and **KSiNb**. The DRIFTS results suggest that HD largely hydrolyzes to HM and TDG upon exposure to these P-PONbs, even under a dry He flow. Reactivity of these 1D materials under humid conditions would likely increase.

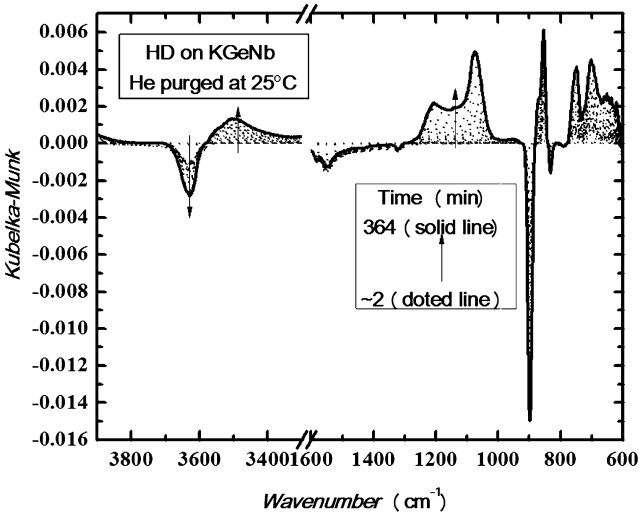

Figure 3. Difference DRIFTS spectra of HD sorption onto **KGeNb**.

Polyanions, $\{[(OH)_2Ti[XNb_{12}O_{40}\text{-}(Ti_2O_2)\text{-}O_{40}Nb_{12}XTi\text{-}(OH)_2]$, where X = Si (1) and Ge (2), were chosen as a model of the **KSiNb** and **KGeNb** polymers. Calculations show that DMMP coordinates to model complexes **1** and **2** via hydrogen bonding. The calculated bonding energies of 23–24 (10–11) kcal mol^{-1} are consistent with this bonding pattern. Furthermore, as a result of this weak interaction, coordination of DMMP only slightly changes the geometry of **1** or **2** (Figure S17 and Table S2). As noted above, this reaction very likely proceeds via a general-base hydrolysis mechanism, the rate-limiting transition state of which involves a water molecule being deprotonated by the P-PONb oxygen atoms forming hydroxide which attacks the electrophilic phosphorus of DMMP. The potassium counter cation and one of the oxo-centers of P-PONb (terminal or bridging) are likely also involved. The subsequent proton transfer to -OCH_3 fragment is expected to be fast. Elucidation of the latter mechanistic details requires dynamic studies and more complex model systems, which are beyond the scope of this paper.

In summary, the newly prepared one-dimensional P-PONb, **KGeNb**, is as active as any known base for hydrolysis of nerve agents and their simulants. Importantly, **KGeNb** is far more reactive than hydroxide alone toward the simulants at the same pH in water. Experimental and calculated data implicate a general-base catalysis mechanism for hydrolysis of DMMP, and by extension, likely the live nerve agents themselves. The P-PONbs remove the CWAs, GD (Soman), GB (Sarin) and HD (mustard) effectively. Hydrolytic breakdown of the CWA proceeds in either solution or the gas phase.

Acknowledgements

C.L.H. thanks the ARO (grant number W911NF-12-1-0136) for support of this work. W.O.G., A.B. and G.W.W. (Programs BB11PHM156 and BA13PHM210) gratefully acknowledge support by the Defense Threat Reduction Agency. We thank Bryan Schindler for help on the DRIFTS experiments.

Keywords: catalysis · chemical warfare agents · decontamination · heteropolyniobates · hydrolysis

How to cite: *Angew. Chem. Int. Ed.* **2016**, *55*, 7403–7407
Angew. Chem. **2016**, *128*, 7529–7533

[1] a) F. M. Raushel, *Nature* **2011**, *469*, 310–311; b) M. Enserink, *Science* **2013**, *341*, 1050–1051; c) M. B. D. Nikitin, P. K. Kerr, A. Feickert, *Syria's Chemical Weapons: Issues for Congress* **2013**, report R42848.

[2] a) N. Sharma, R. Kakkar, *Adv. Mater.* **2013**, *4*, 508; b) N. Munro, *Environ. Health Perspect.* **1994**, *102*, 18–37; c) W. W. George in *Nanoscale Materials in Chemistry: Environmental Applications*, *Vol. 1045*, American Chemical Society, Washington, DC, **2010**, pp. 125–136.

[3] "Introduction to and Mitigation of Psychological Effects of Weapons of Mass Destruction (WMD)": R. H. Pastel, E. C. Ritchie in *Psychological Responses to the New Terrorism: A NATO-Russia Dialogue*, IOS Press, Amsterdam, **2005**, pp. 9–24.

[4] a) Y. J. Yang, K. Kim, O. G. Tsay, D. A. Atwood, D. G. Churchill, *Chem. Rev.* **2015**, *115*, PR1–PR76; b) Y. C. Yang, J. A. Baker, J. R. Ward, *Chem. Rev.* **1992**, *92*, 1729–1743.

[5] A. N. Bigley, F. M. Raushel, *Biochim. Biophys. Acta Proteins Proteomics* **2013**, *1834*, 443–453.

[6] a) G. W. Wagner, P. W. Bartram, *J. Mol. Catal. A* **1999**, *144*, 419–424; b) G. Lunn, E. B. Sansone, *Appl. Biochem. Biotechnol.* **1994**, *49*, 165–172; c) L. Bromberg, T. A. Hatton, *Polymer* **2007**, *48*, 7490–7498; d) L. Chen, L. Bromberg, J. A. Lee, H. Zhang, H. Schreuder-Gibson, P. Gibson, J. Walker, P. T. Hammond, T. A. Hatton, G. C. Rutledge, *Chem. Mater.* **2010**, *22*, 1429–1436; e) H. Morales-Rojas, R. A. Moss, *Chem. Rev.* **2002**, *102*, 2497–2522; f) L. Bromberg, T. A. Hatton, *Ind. Eng. Chem. Res.* **2007**, *46*, 3296–3303; g) L. Bromberg, H. Zhang, T. A. Hatton, *Chem. Mater.* **2008**, *20*, 2001–2008; h) Y. Xie, B. N. Popov, *Anal. Chem.* **2000**, *72*, 2075–2079; i) T. J. Bandosz, M. Laskoski, J. Mahle, G. Mogilevsky, G. W. Peterson, J. A. Rossin, G. W. Wagner, *J. Phys. Chem. C* **2012**, *116*, 11606–11614; j) G. W. Wagner, G. W. Peterson, J. J. Mahle, *Ind. Eng. Chem. Res.* **2012**, *51*, 3598–3603; k) G. W. Peterson, J. A. Rossin, *Ind. Eng. Chem. Res.* **2012**, *51*, 2675–2681; l) A. Kiselev, A. Mattson, M. Andersson, A. E. C. Palmqvist, L. Österlund, *J. Photochem. Photobiol. A* **2006**, *184*, 125–134; m) L. Bromberg, W. R. Creasy, D. J. McGarvey, E. Wilusz, T. A. Hatton, *ACS Appl. Mater. Interfaces* **2015**, *7*, 22001–22011.

[7] a) S. Y. Moon, Y. Liu, J. T. Hupp, O. K. Farha, *Angew. Chem. Int. Ed.* **2015**, *54*, 6795–6799; *Angew. Chem.* **2015**, *127*, 6899–6903; b) M. J. Katz, J. E. Mondloch, R. K. Totten, J. K. Park, S. T. Nguyen, O. K. Farha, J. T. Hupp, *Angew. Chem. Int. Ed.* **2014**, *53*, 497–501; *Angew. Chem.* **2014**, *126*, 507–511; c) E. López-Maya, C. Montoro, L. M. Rodríguez-Albelo, S. D. A. Cervantes, A. A. Lozano-Pérez, J. L. Cenís, E. Barea, J. A. R. Navarro, *Angew. Chem. Int. Ed.* **2015**, *54*, 6790–6794; *Angew. Chem.* **2015**, *127*, 6894–6898; d) J. E. Mondloch, M. J. Katz, W. C. Isley III, P. Ghosh, P. Liao, W. Bury, G. W. Wagner, M. G. Hall, J. B. DeCoste, G. W. Peterson, R. Q. Snurr, C. J. Cramer, J. T. Hupp, O. K. Farha, *Nat. Mater.* **2015**, *14*, 512–516.

[8] Toxicology and Carcinogenesis Studies of Dimethyl Methylphosphonate(CAS No. 756-779-6) in F344/N Rats and B6C3F$_1$ Mice (Gavage Studies), National toxicology program, U.S. Department of Health and Human Services, **1987**, Technical Report Series 323.

[9] Y. Liu, A. J. Howarth, J. T. Hupp, O. K. Farha, *Angew. Chem. Int. Ed.* **2015**, *54*, 9001–9005; *Angew. Chem.* **2015**, *127*, 9129–9133.

[10] a) M. K. Kinnan, W. R. Creasy, L. B. Fullmer, H. L. Schreuder-Gibson, M. Nyman, *Eur. J. Inorg. Chem.* **2014**, 2361–2367; b) F.-J. Ma, S.-X. Liu, C.-Y. Sun, D.-D. Liang, G.-J. Ren, F. Wei, Y.-G. Chen, Z.-M. Su, *J. Am. Chem. Soc.* **2011**, *133*, 4178–4181;

c) D. M. Mizrahi, S. Saphier, I. Columbus, *J. Hazard. Mater.* **2010**, *179*, 495 – 499; d) N. M. Okun, J. C. Tarr, D. A. Hilleshiem, L. Zhang, K. I. Hardcastle, C. L. Hill, *J. Mol. Catal. A* **2006**, *246*, 11 – 17; e) N. M. Okun, T. M. Anderson, C. L. Hill, *J. Mol. Catal. A* **2003**, *197*, 283 – 290; f) F. Carniato, C. Bisio, R. Psaro, L. Marchese, M. Guidotti, *Angew. Chem. Int. Ed.* **2014**, *53*, 10095 – 10098; *Angew. Chem.* **2014**, *126*, 10259 – 10262.

[11] a) T. Yamase, M. T. Pope in *Nanostructure Science and Technology*, *Vol. 2* (Ed.: D. J. Lockwood), Kluwer/Plenum, New York, **2002**; b) M. T. Pope in *Comprehensive Coordination Chemistry II: From Biology to Nanotechnology*, *Vol. 4* (Ed.: A. G. Wedd), Elsevier, Oxford, **2004**, pp. 635 – 678; c) H. N. Miras, J. Yan, D.-L. Long, L. Cronin, *Chem. Soc. Rev.* **2012**, *41*, 7403 – 7430; d) H. Lv, Y. V. Geletii, C. Zhao, J. W. Vickers, G. Zhu, Z. Luo, J. Song, T. Lian, D. G. Musaev, C. L. Hill, *Chem. Soc. Rev.* **2012**, *41*, 7572 – 7589; e) C. L. Hill, in *Chem. Rev. Vol. 98*, *No. 1*, **1998**, pp. 1 – 390.

[12] a) M. R. Antonio, M. Nyman, T. M. Anderson, *Angew. Chem. Int. Ed.* **2009**, *48*, 6136 – 6140; *Angew. Chem.* **2009**, *121*, 6252 – 6256; b) M. Nyman, T. M. Alam, F. Bonhomme, M. A. Rodriguez, C. S. Frazer, M. E. Welk, *J. Cluster Sci.* **2006**, *17*, 197 – 219; c) M. Nyman, *Dalton Trans.* **2011**, *40*, 8049 – 8058; d) E. M. Villa, D. C. André Ohlin, D. Edina Balogh, D. Travis, M. Anderson, D. May, D. Nyman, P. W. H. Casey, *Angew. Chem. Int. Ed.* **2008**, *47*, 4844 – 4846; *Angew. Chem.* **2008**, *120*, 4922 – 4924; e) E. Balogh, T. M. Anderson, J. R. Rustad, M. Nyman, W. H. Casey, *Inorg. Chem.* **2007**, *46*, 7032 – 7039.

[13] M. Nyman, F. Bonhomme, T. M. Alam, M. A. Rodriguez, B. R. Cherry, J. L. Krumhansl, T. M. Nenoff, A. M. Sattler, *Science* **2002**, *297*, 996 – 998.

[14] F. Bonhomme, J. P. Larentzos, T. M. Alam, E. J. Maginn, M. Nyman, *Inorg. Chem.* **2005**, *44*, 1774 – 1785.

[15] CCDC 1453051 contains the supplementary crystallographic data for this paper. These data can be obtained free of charge from The Cambridge Crystallographic Data Centre.

[16] W. P. Jencks, *Catalysis in Chemistry and Enzymology*, McGraw-Hill, New York, **1969**.

[17] C. A. Bunton, S. Diaz, *J. Org. Chem.* **1976**, *41*, 33 – 36.

Received: February 15, 2016
Revised: March 17, 2016
Published online: April 9, 2016

